see file

CLM-P 130

CLM-P 130

United Kingdom Atomic Energy Authority

RESEARCH GROUP

Preprint

A ONE-MEGAJOULE LOW-INDUCTANCE CAPACITOR BANK FOR NUCLEAR FUSION RESEARCH

N. R. McCORMICK

Culham Laboratory
Abingdon Berkshire

1967

UNCLASSIFIED
(Approved for publication)

CLM - P 130

A ONE-MEGAJOULE LOW-INDUCTANCE CAPACITOR BANK FOR NUCLEAR FUSION RESEARCH

by

N.R. McCORMICK
(Submitted for publication in Proc. Inst. Elec. Engs.)

A B S T R A C T

This low-inductance capacitor bank was constructed at the Culham Laboratory of the U.K.A.E.A. for research on high-density theta-pinch plasmas. The bank has a maximum voltage of 40 kV and an inductance - including a current collector shaped to feed a 2 metre coil - of 5.6 nH. When discharged into a coil 2 metres long and 10 cm diameter, the resultant current waveform is oscillatory with Q = 4.5, half-period 12 μsec, and peak current 12 MA, generating a peak magnetic field of 76 kG.

The bank comprises 448 parallel discharge circuits separately switched by atmospheric swinging-cascade sparkgaps. The trigger system comprises a cascade connection of high-voltage pulse generators: a single master generator triggers eight sub-master generators, each of which produces 56 output pulses for triggering the main sparkgaps. Each trigger-pulse generator uses a swinging-cascade sparkgap pressurised with SF_6 to 25 lb/sq.in. above atmospheric. The trigger system is pulse-charged in 2 μsec. The overall time-spread in operation of the main sparkgaps is less than 35 nsec, of which the trigger-generator sparkgaps contribute not more than 10 nsec.

U.K.A.E.A. Research Group,
Culham Laboratory,
Abingdon,
Berks.

December 1966 (ED)

C O N T E N T S

1. INTRODUCTION

One approach to the problem of controlled nuclear fusion is the theta-pinch discharge, so-called because of the direction of current flow in increasing θ direction in a cylindrical block of plasma. Current in an external single-turn coil induces an opposite surface current in a pre-ionized plasma, as in Fig.1, causing plasma heating by radial compression under the pressure of the magnetic field confined between the coil and plasma. Research is directed towards the containment of the hot compressed plasma long enough to achieve a net energy gain from nuclear fusion reactions. In the most favourable case of a 50% deuterium-tritium mixture, it is calculated that the plasma must be heated to a temperature of 10,000 eV (10^8 ^{o}K) and held together long enough for about 1% of the particles to undergo thermonuclear reactions. At a particle density of 10^{17} cm^{-3} this demands containment times of at least a millisecond. The megajoule bank was constructed to extend theta-pinch research at this Laboratory (previously at AWRE) to larger gas volumes and duration of current flow in order to study the problem of plasma stability and containment.

Ideally, the compressing magnetic field would rise with the maximum possible initial rate of rise (for plasma heating) to a specified peak value, and subsequantly would remain at the peak value long enough for experimental observation of plasma containment. These characteristics would be produced by a capacitor bank designed to feed into the particular thetatron coil with the highest possible voltage/inductance ratio[1], clamped at current peak (voltage zero) to produce a slow fall of magnetic field. In the relatively primitive state of clamp-switch technology at the time the megajoule bank was conceived it was considered wiser to design for an unclamped (oscillatory) discharge and to add clamp facilities later: the values of $\frac{dH}{dt}$ $(t = 0)$, $\hat{H}$ and period of oscillation are then related, and the design becomes a selection of bank parameters to achieve acceptable values of $\dot{H}$, $\hat{H}$ and T within a framework imposed by the range of coil dimensions to be used and by cost (and therefore maximum stored energy). One megajoule represents an increase in stored energy some 20-fold relative to our previous capacitor banks.

The megajoule bank has been operating reliably since April, 1964. It is comparable in performance with other capacitor banks for theta-pinch research at Julich[2] (600 kJ, 30 kV), Munich[3] (1.5 MJ, 30 kV, or 2.25 MJ, 40 kV for reduced life), NRL, Washington[4,5,6] (2 MJ, 20 kV, plus 3 MJ, 5 kV clamp) and Los Alamos[7] (500 kJ, 50 kV, plus 3 MJ, 20 kV clamp). Passive clamp switches have recently been added to the Culham bank, and are described elsewhere[8].

2. BANK PARAMETERS

A high-energy low-inductance capacitor bank necessarily comprises many parallel separately-switched discharge circuits feeding into a common collector and load coil. The circuit may be simplified, as in Fig.2, to the discharge of the total bank capacitance C_B through a series inductance L and resistance R, where L is the sum of the bank inductance L_B, collector inductance L_C and field-coil inductance L_F, and similarly R is the sum of R_B, R_C and R_F. L_F is the effective inductance of the coil containing a conducting plasma, and will depend on the diameter d of the plasma surface:

$$L_F = L_{FV}\left(1 - \frac{d^2}{d_1^2}\right)$$

where d_1 is the inner coil diameter and L_{FV} the vacuum inductance of the coil $\pi^2 d_1^2$ and ℓ is the coil length. Initially:

$$L_F\ (t = 0) = L_{FO} = L_{FV}\left(1 - \frac{d_2^2}{d_1^2}\right) = \lambda L_{FV}$$

where d_2 is the inner diameter of the discharge tube, and $\lambda < 1$, usually about 0.5. Usually the discharge of the capacitor bank is only lightly damped, in which case it is characterised by:

$$\frac{dH}{dt}\ (t = 0) = \dot{H}_o = \frac{4\pi}{10\ell} \cdot \frac{V_B}{(L_B + L_C + \lambda L_{FV})} \quad \text{oersted sec}^{-1}$$

$$\hat{H}_1 = \frac{4\pi}{10\ell}\ V_B \sqrt{\frac{C_B}{(L_B + L_C + L_{FV})}} \times \eta_1 \text{ oersteds}$$

$$\text{Period } T = 2\pi \sqrt{C_B\ (L_B + L_C + L_{FV})} \quad \text{seconds}$$

$\hat{H}_1$ is the peak value of magnetic field on the first half cycle, $\eta_1 = \exp(-\pi/4Q)$ is the decay factor in a damped oscillatory discharge at first current peak and $Q = \frac{1}{R}\sqrt{\frac{L}{C}}$.

Equation (1) may be re-written:

$$\dot{H}_O = \frac{4\pi}{10} \frac{1}{\left(\frac{1}{k} + \frac{\pi^2 d_1^2 \lambda}{V_B}\right)} \quad \text{oersteds sec}^{-1}$$

where

$$k = \frac{V_B}{\ell(L_B + L_C)} \quad \text{amperes cm}^{-1}\ \text{sec}^{-1} \ .$$

The value of k is the rate of rise of current per unit width of collector output when terminated by a short circuit, i.e. k is a characteristic of the bank plus collector as a whole. There is an upper limit to the value of k determined by the dielectric strength of insulating materials. The value of k will be determined by the techniques used in circuit construction and by the utilization by the discharge circuits of the available volume around the load coil. With present techniques it is not difficult to achieve $k = 10^{11}$ amp cm^{-1} sec^{-1}. For a particular load inductance L_{FV}, the value of $\dot{H}_O$ approaches the upper limit $\frac{4\pi k}{10}$ when the bank voltage is chosen high enough to ensure that $(L_B + L_C) \gg \lambda L_{FV}$, i.e. when $V_B \gg k\,\pi^2 d_1^2 \lambda$. In these circumstances the bank voltage is high enough to ensure that the combined bank and collector inductance, although as small as possible, swamps the field-coil inductance and, effectively, the bank discharges into a short circuit[1].

The megajoule design is a selection of parameters to produce acceptable values of H_O, $\hat{H}_1$ and T within the overall limitations imposed by a stored energy of the megajoule and a value of k chosen to permit relatively low stresses in the discharge circuit connections and a reasonable access to the coil for experiments. Fig.3 shows $\dot{H}_O$, $\hat{H}_1$, and T plotted as a function of V_B for a stored energy of 10^6 joules and $k = 0.4 \times 10^{10}$ amp cm^{-1} sec^{-1}. The value of λ is taken as 0.5. The choice of $V_B = 40$ kV represents a reasonable compromise, which has the

advantage that, using high-impedance (50 Ω) cables for interconnections, the surface electric stresses are low enough to permit the use of simple and inexpensive cable terminations without stress grading. 40 kV defines the value of C_B at 1250 μF and $(L_B + L_C)$ at 5 nH: these are approximate values intended as a guide for the more detailed design.

The design philosophy was to use many parallel discharge circuits to secure the advantages of low electrical and mechanical stresses and low switch loading[9]. Under these conditions atmospheric sparkgaps can give precise and repeatable breakdowns for some thousands of operations before needing maintenance. Empirical tests on a single circuit, with the period of oscillation and Q adjusted to correspond to the discharge of the whole bank (T = 28 μsec and Q = 10), gave a sparkgap life exceeding 5000 discharges with C = 3 μF. This corresponds per circuit to a stored energy of 2.4 kJ, stored charge of 0.12 coulombs, and an ampere-second duty at Q = 10 of 1.2 coulombs. The number of parallel circuits was chosen to be 448 to give many alternative groupings of discharge circuits both for construction and triggering, giving a nominal total stored energy of 1.072 MJ. If it is assumed that $L_B = L_C$, approximately, the required inductance per circuit is 1.15 μH.

3. THE MAIN DISCHARGE CIRCUITS

3.1 The Main Sparkgaps

The atmospheric swinging-cascade sparkgap possesses many advantages for use as a high-voltage switch in capacitor banks[9]: its mode of operation involves the predictable breakdown of overvolted sparkgaps and is well understood; the time-spread in operation between many similar gaps subjected to identical trigger pulses can be predicted approximately and it is not difficult to achieve a time spread less than 20 nsec; with suitable circuit parameters the sparkgaps will work down to less than half their static breakdown voltage without the need for a variable gas pressure; and the impedance of trigger and output cables are unrelated in the mode of operation and may be chosen independently. The mode of

operation has been described in detail elsewhere[9,10], but will be summarised with reference to Fig.4, which represents a basic capacitor-discharge circuit. The sparkgap comprises two series component gaps with the common (trigger) electrode held at a steady (bias) voltage intermediate between the two outer electrodes such that the component gaps are equally stressed. The trigger pulse is applied to the common electrode and initiates breakdown of the series component gaps in sequence. If the trigger pulse is opposite in polarity to V_W, then gap 1 should breakdown first, followed by gap 2 when the trigger-electrode voltage rises towards V_W. Two conditions must be satisfied: gap 1 should breakdown first under the overvoltage due to the applied trigger pulse; and there should subsequently be sufficient overvoltage to breakdown gap 2. These conditions, with the choice of safety factor, determine the optimum gap ratio $q(= \frac{\ell_2}{\ell_1 + \ell_2})$ and the working voltage range for particular circuit parameters. The rise of voltage across gap 2 after breakdown of gap 1 occurs due to the charging of capacitor C_2 through L; with less than critical damping the voltage across C_2 will swing beyond V_W, which in effect permits a larger working voltage range. For small damping, the trigger-cable impedance should be appreciably larger than $\frac{1}{2}\sqrt{\frac{L}{C}}$, and the half-period of the overswing oscillation appreciably longer than the fall-time of spark-channel resistance (10–20 nsec)[11,12].

An extra electrode has been added between the trigger and output electrodes, as shown in Fig.5, connected to the earth return through 24 k Ω. This serves to isolate the swinging-cascade section from transients appearing at the output electrode prior to triggering. Such transients could be caused by the discharge of a θ pre-ionization bank or by the spurious breakdown of another main sparkgap. Since the isolating electrode is held at earth potential the stress in the last gap is independent of the polarity of the transients. The isolating gap has a static breakdown voltage of 12 kV: on triggering, when breakdown of gap 2 occurs, the voltage across C_2 appears across the 24 k Ω resistor and hence across the isolating gap. Fig.6 shows typical voltage waveforms at the sparkgap electrodes during triggering, in which can be seen discontinuities representing

breakdown of the three component gaps: similar records taken as a routine check on each sparkgap after circuit assembly gave an overall time-spread in operation between the 448 main gaps of less than 25 nsec.

A cross-section drawing showing mechanical details of the main sparkgap is shown in Fig.7. The electrodes are moulded axially in 6"-diameter silica-loaded epoxy insulators provided with annular grooves to increase the flash-over path length. Annular spacers are provided to limit external noise, but each spacer has six $\frac{3}{8}$"-diameter radial holes for ventilation to the atmosphere. The assembly is clamped to a polythene-insulated earth-return tray, which provides for easy access; also the resultant asymmetric magnetic field gives some blow-out of the arc away from the earth tray. Connection to the electrodes is by coaxial cable which has sufficient flexibility to take up manufacturing and assembly tolerances. Gap lengths are held within ± .005" between sparkgaps. The gap ratio is 0.4 and the safety factor is 1.5.

An irradiating sparkgap assembly fits into the trigger electrode and irradiates the component gaps of each main sparkgap through 1/16"-diameter axial holes in the trigger and isolating electrodes. The trigger pulse must breakdown the irradiating gap before reaching the trigger electrode, and the charging current into the swinging-cascade capacitor C_2 provides the U-V illumination.

3.2 Circuit Details

All 448 discharge circuits are identical, with details as shown in Fig.5. The 1.5 μF main-discharge capacitors are designed for a life of at least 10^5 discharges in fast oscillatory discharge with voltage reversal not exceeding 80%. All main-discharge interconnecting cables are standard-quality 50 ohm coaxial cable, 1/8" diameter conductor, multiple cables being used to obtain the required low inductance. High impedance cables were used partly because of their ready availability, and partly because the relatively low surface electric field strength at 40 kV permits the use of inexpensive cable terminations: the cover and braid of the cable are stripped back about 4 inches and an elementary stress

shield is clamped beneath the braid to shield stray wire ends. The capacitors and sparkgaps for each circuit are mounted horizontally in line (actually 2^{o} to the horizontal) on timber racks, each holding 14 circuits, as shown in photograph of the top floor of the bank in Fig.26.

The swinging-cascade capacitor (C_2) is formed by two 6-ft lengths of 50 ohm coaxial cables doubled on themselves as indicated in Fig.5 to avoid free high-voltage cable ends. The 1 μH inductor provides a d.c. charging connection to these cables, by-passing the irradiating gap, but presents a high impedance to the trigger pulse. The 5 ohm series resistor limits the amplitude of current fed back into the trigger system after the main gap has fired and so controls the rate of erosion of the electrodes of the irradiating gap. The 5000 pF blocking capacitor limits the energy flow into the trigger system from the main capacitors after sparkgap breakdown: the spurious breakdown of one main sparkgap cannot then cause an appreciable change in the trigger-electrode bias voltage of all the other main gaps inter-connected via the same trigger-pulse generator. The 27-MΩ bleed resistor provides the d.c. charging path for the bias-voltage supply to the trigger electrode.

It is essential to ensure that a short-circuit fault in one discharge circuit does not initiate the uncontrolled breakdown of the whole bank. The most common fault is the spurious breakdown of a main sparkgap, which is most likely to occur during charging of the bank following a period of shut down. This can feed transients to other circuits via either the collector or the trigger system. At the collector the single set of main cables carrying the fault transient is loaded by all the other main cables, and the the whole collector capacitance; where there are many parallel circuits the resulting attenuation will be so high that there should be no difficulty in setting the isolating gap of the main sparkgaps to provide adequate protection. Similar loading must be arranged in the trigger system to hold the potential of the trigger electrodes steady against fault transients.

The parallel damping resistor Rd approximately matches the impedance of the main collector cables, and acts to damp out multiple transits of the switching transients along the main cables. Although the matching is not perfect, the resultant ripple on the voltage waveform at the collector is less than ± 20% of the mean (cosine) waveform, and falls effectively to zero within 3 μsec.

4. THE TRIGGER SYSTEM

4.1 Trigger-Pulse Generators

Pulse generators necessarily comprise an energy (discharge) source, switch, and load impedance. In a capacitor-bank the trigger discharge source may comprise high-voltage low-inductance capacitors, or alternatively cables of a suitable length to generate the required duration of trigger pulse; the switch is invariably a high-voltage low-inductance sparkgap; and the load impedance is formed by the parallel connection of the trigger cables feeding the main sparkgaps. Low inductance is a prerequisite for the generation of a large number of fast-rising high-voltage trigger pulses: the lower the circuit impedance the slower the rise of output pulse, for a given sparkgap inductance. As the number of parallel circuits increases it becomes increasingly difficult to generate high-voltage pulses with sufficient rate of rise to ensure small jitter in the main sparkgaps. Also the mechanical dimensions of the sparkgap assembly becomes something of an embarrassment. There comes a point at which it is preferable to use more than one pulse generator, even though this introduces the problems of ensuring precise and consistent triggering and freedom from spurious breakdowns (important because each pulse generator then controls a sizable section of the bank).

The symmetrical arrangement of trigger-pulse generator shown schematically in Fig.8(a), with cables feeding radially to the sparkgap switch, is an obvious step towards identical circuits. The discharge cables we call trigger-discharge cables, and the output cables trigger-pulse cables. Assuming that most of the inductance lies in the spark, the switch inductance is proportional to the gap length but only to the log of the ratio of outer to inner diameters. This leads

to the arrangement in Fig.8(b), where the sparkgap is pressurised to reduce its length and to speed the fall of voltage, and connection between the gap and the cables is made by two circular trays having the closest spacing permitted by the dielectric strength of the insulation. The outer diameter is chosen to accommodate the cable terminations around the perimeter. In a system comprising a single pulse-generator the trigger-discharge cables would be pulse-charged from a marx generator to overvolt and breakdown the sparkgap on the voltage rise. Where there are two or more pulse generators (sub-master trigger-pulse generators) they must be triggered from a common (master) pulse generator to achieve the required triggering precision of a few nanoseconds. Fig.8(c) shows the design modified to incorporate a trigger electrode for operation in the swinging-cascade mode.

Fig.9 shows a cross-section drawing of a sub-master sparkgap assembly intended for use up to 80 kV and tested up to 100 kV. The gaseous insulant is SF_6 at a normal pressure of 25 lbs/sq.in. above atmospheric (the gap operates satisfactorily over a pressure range 15-35 lb/sq.in.). The gap ratio is 1/3 for operation in the swinging-cascade mode, with gap lengths of .130" and .065" held within .002" manufacturing tolerance. An irradiating sparkgap is connected (in series with a C-R circuit to limit the current) between the trigger electrode and earth: the gap length must be less than .010" to ensure breakdown of the irradiating gap first. The trigger-discharge and trigger-pulse cables are identical (50 Ω) and have their ends moulded in conical form, increasing first to 1¾" diameter, backed by a copper spinning, then tapering in a machined surface that fits closely in a corresponding female taper in a polythene ring shrunk inside the sparkgap earth ring. The increase in diameter reduces the surface electric field and the close fit between tapers provides a difficult breakdown path. Fig.10 shows an assembled sub-master trigger-pulse generator.

The equivalent circuit of a pulse generator must include the capacitance between the connecting trays as shown in Fig.11. Whilst for the master sparkgap the tray capacitance can be neglected, for the sub-master sparkgap it is about

5000 pF and must be taken into account. An output pulse from a sub-master gap is shown in Fig.12, which, by comparison with analogue-computer curves corresponding to a range of gap inductances (assuming all the inductance to be concentrated in the spark) gave a nearest approximation of 25 nH for the gap inductance. Fig.13 shows a trigger pulse at a main sparkgap across the swinging-cascade capacitance.

4.2 The Complete Trigger System

A schematic diagram showing the overall circuit of the bank is shown in Fig.14 and a more detailed circuit of the trigger system in Fig.15. The single master trigger-pulse generator triggers eight sub-master trigger-pulse generators, each of which produces 56 output pulses for triggering main sparkgaps. The cascade connection of trigger-pulse generators is pulse charged in 2 μsec from two marx generators and is triggered at the peak of the charging waveform. In the absence of triggering the pulse-charging voltage decays with a 15 μsec time constant. The system is initiated by a d.c.-charged (40 kV) blumlein-type pulse generator which produces 3 trigger-pulses, two of which trigger the marx generators and the third is delayed by two microseconds (in coaxial cable) before triggering the master sparkgap. The blumlein pulse generator is triggered by a chain of thyratron pulse generators starting with a 200-volt trip pulse generated in the control area in synchronism with the measuring equipment for plasma-physics experiments.

The success of the trigger-system design rests on the reliability of the trigger-generator sparkgaps, particularly the sub-master sparkgaps since each triggers one eighth of the whole bank. Operation of the sparkgaps in the swinging-cascade mode has ensured consistent triggering, and a combination of pulse-charging and use of an electron-attaching gas has given, to date, complete freedom from spurious breakdowns under normal operating conditions. Inevitably there will be short-circuit faults to ground in the course of time (for example, cable breakdowns) which will result in a failure of one eighth of the whole bank to trigger. Such faults are likely to be rare, but can result in dangerous overvoltages across bank capacitors: protection circuits should aim to detect the removal of voltage

from the trigger-generator sparkgaps before the normal triggering time spread, and to suppress the trigger-pulse to the system or, alternatively, to dump the remainder of the energy in the trigger system quickly. Whilst it should be possible to provide such protection up to an instant close to the normal triggering time, this has not been incorporated to date.

Some parts of the trigger system must use sparkgaps or thyatrons which are subjected to a steady stress, and it would be unrealistic to rely on a complete absence of spurious breakdowns. If either of the two marx generators should operate spuriously, the corresponding part of the trigger system would charge without triggering. If the blumlein pulse generator or an earlier stage should operate spuriously, this would merely trigger the system normally providing that the system were charged to above about three quarters of its normal voltage. Such spurious breakdowns are most likely to occur after a period out of use, and the trigger system is always operated independently several times after a shut down period to ensure that the sparkgaps are stable. Also, in normal operation the bank is charged first to ensure that the main sparkgaps are within their operating range when the trigger system is charged.

Each sub-master trigger-pulse generator has 64 sets of cables: 56 trigger-pulse cables feed main sparkgaps, 2 are used for monitoring, and 6 connect to low-inductance loading capacitors. The loading capacitors hold the potential of the trigger-pulse cables steady against feed-through of the pulse-charging waveform through the capacitance between sparkgap trays. The master sparkgap needs no loading capacitor because the tray capacitance is negligible. Fig.16 shows the pulse-charging waveforms of the master and sub-master trigger-pulse generators. Fig.17 shows five superimposed exposures of the trigger-electrode voltage waveform of a sub-master sparkgap: from similar waveforms for all eight sub-master sparkgaps the overall time spread in operation of the trigger system was measured to be less than 10 nsec.

The monitoring system is intended to give all essential information on the performance of the trigger system on two polaroid records, which reasonably can be

taken on every firing of the bank. It is required to know that each generator (a) charges (b) triggers correctly. One oscilloscope contains nine 1½" diameter cathode ray tubes, each of which displays the charging-voltage waveform of one generator. The other oscilloscope displays voltage spikes derived from the leading edge of trigger pulses from each pulse generator, delayed by successively increasing times of 50 nsec, to give a succession of spikes on an 0.5 μsec time base, which can be resolved in position to within about 10 nsec. Fig.18 is a record of the charging waveforms, and Fig.19 shows 20 successive sets of voltage spikes. Fig.20(a) shows the chopping circuit used to derive the voltage spikes from the trigger pulses, and Fig.20(b) the input circuit to the oscilloscope.

Waveforms at all major points in the system may be selected for detailed monitoring. Resistance dividers are used throughout. The high-voltage arm of the divider consists of composition resistor blocks of sufficient length to withstand the voltage (at 10 kV/inch manufacturer's rating) and the lower arm from a wafer of the same material, all contained in a coaxial screening can. The transient response depends on the resistance value and connecting lead arrangements: for a 1000 Ω, 60-kV divider with short leads the output pulse rise-time is about 5 nsec for a 1 nsec input rise-time.

5. THE COLLECTOR

The purpose of the collector is to make a low-inductance connection between the discharge circuits and the coil. The collector consists of two parallel plates, separated by a thin layer of insulation and shaped to accommodate the cable terminations at the input and feed into the coil at the output. For theta-pinch experiments the magnetic field should have a high degree of uniformity: for example, a gradient of 0.1 gauss cm^{-1} across a diameter in a 100 kG field causes a 1 keV plasma to drift to the wall of a 10 cm diameter tube in 100 μsec[13]. Of the four principal causes of field nonuniformity, which have been discussed in detail elsewhere[13], the largest effect is due to the converging lines of current flow resulting from the reduction in width of the collector between cables and coil.

This may be overcome by feeding the current into the coil through a parallel-sided section or tab: the longer the tab the more uniform the magnetic field, but the higher the collector inductance. Fig.21 shows a plan view of the collector used in the megajoule bank, feeding a 2-metre coil, and Fig.22 a photograph of the collector and experimental area.

When the bank is discharged the magnetic field between the conducting surfaces of the collector plates subjects the plates to an explosive impulse which must be contained. Movement of the plates can cause burning at current contacts, and the impulsive stresses can cause deterioration of insulation. The energy imparted to the plates may be reduced by concentrating mass near the conducting surfaces; but even using lead an appreciable thickness is required, which is undesirable in the vicinity of the coil (where it is most needed) because of possible bending of magnetic field lines due to the presence of conducting surfaces. In the megajoule bank the collector plates are formed from 4"-thick aluminium plates, backed by ½" rubber sheet to reduce peak stresses, and then by concrete blocks, all clamped together by insulated steel tie bolts passing through the collector plate[14,15]. A cross-section at one of the tie bolts is shown in Fig.23. Energy is absorbed in multiple transits of the stress waves in the concrete. In the centre section, where the stresses are highest, the concrete is moulded in glass-fibre boxes strengthened by glass-fibre reinforcing rods. The outer blocks are cantilevered from the centre sections, using post-tensioned steel tie bolts, to give access to under-floor ducting.

The main cables feeding from the discharge circuits connect along the rear face of the collector in low-inductance terminations resembling interlocking fingers, as can be seen in the photograph of the rear of the collector during assembly, in Fig.24.

6. THE COMPLETE BANK

The capacitor bank is constructed on a steel framework leaving the ground floor free for an experimental area, as shown in the schematic diagram in Fig.25. The capacitor racks are mounted two-floors high on the structure, with the output

cables feeding vertically down to the collector. Fig.26 shows a photograph of the top floor of capacitor racks, with the master trigger-pulse generator on top and four sub-master generators along one side; the other four are mounted along the opposite side. An area approximately 60 ft × 40 ft of the ground floor is covered with copper sheet to form a reference earth for the bank during discharge by virtue of its capacitance to ground (the copper floor is itself earthed through wires, which are too inductive to be effective during discharge of the bank). The capacitor bank has one main earth connection to the copper floor at the collector; other earth connections are provided at each rack for safety during maintenance, but are made inductive to limit circulating currents. The copper floor extends to the screened cubicles outside the bank area, and makes connection to them at floor level along their full length. Signal cables for plasma diagnostics are run in copper pipes in ducts beneath the copper floor, with separate pipes for low, medium and high-level signals. Signal cables for bank monitoring, where the signal level is some hundreds of volts, are routed on the bank framework. Comprehensive controls and safety interlocks are provided.

7. BANK PERFORMANCE

The discharge of a single circuit, one rack and $\frac{1}{8}$-bank into a short circuit and into various load inductances gave the values of inductance and resistance per rack to be approximately 93 nH and 6 mΩ, and hence the inductance and resistance of the whole bank, up to and excluding the collector, to be 2.9 nH and 0.19 mΩ. Discharge of the whole bank into a 5 nH coil 2 metres long and 10 cm diameter gave a ½-period of 12 μsec and hence a total inductance of 10.7 nH, leaving 2.8 nH as the collector inductance. From the measured Q of 4.5 the calculated series resistance is 0.48 mΩ when account is taken of the damping effect of the parallel resistors at the collector. The resultant equivalent circuit is shown in Fig.27. The resistance of coil plus collector is too high to be accounted for by an approximate calculation of skin resistance: the difference may arise from the voltage dependence of the parallel resistors across the collector, or from the high-current contact in the collector.

Since commissioning, the bank has been discharged more than 12,000 times.

8. CONCLUSION

Although intended primarily for theta-pinch research, the megajoule capacitor bank provides a high-current low-inductance discharge facility likely to be generally useful for experiments on high-temperature plasmas. The cascade trigger system, which is capable of extension should larger banks be required in the future, has demonstrated a technique for producing several hundred fast-rising high-voltage trigger pulses with a time-spread between pulses of less than 10 nsec.

9. ACKNOWLEDGEMENTS

The author wishes to acknowledge the contribution made to the work on the megajoule bank by many colleagues, in particular Mr R.J. Hucklesby on mechanical design, Messrs. T. Quayle, P.D. Wilcock and D.V. Bayes on the main-discharge circuits and the control and protection systems, and Messrs. F.J. Kivlin, D. Markins, and L. Firth on the trigger system and bank-monitoring facilities.

The author also acknowledges the impetus given to the project by Professor K.W. Allen, the control of the mechanical engineering design and manufacture by Mr A.J. Marriott at A.W.R.E., and helpful discussions throughout with Dr G.B.F. Niblett under whose overall responsibility for theta-pinch research the work was carried out.

This paper is published by permission of the Director of the Culham Laboratory of the United Kingdom Atomic Energy Authority.

10. REFERENCES

1. FITCH, R.A. 'Rapid heating for controlled fusion research', Proc. IEE, 1959, 106A, Suppl. 2, p.177.

2. FAY, H. and ANGER, W. 'A 600 K Joule set-up for fast magnetic compression experiments', 2nd Symposium on Engineering Problems in Thermonuclear Research, Paris, 162, p.65.

3. KNOBLOCH, A. 'The 2.6 MJ capacitor bank at Garching - arrangement and collector system', Proc. 3rd Symposium on Engineering Problems in Thermonuclear Research, Munich, 1964, p.55.

4. GRIEM, H.R., ELTON, R.C., KOLB, A.C., LUPTON, W.H. and HINTZ, E. 'The Pharos experiment for producing high-temperature plasma', Rept. NRL Prog. October 1963, p1.

5. KOLB, A.C. and LUPTON, W.H. 'A pulsed field plasma experiment - Pharos', Int. Conf. on High Magnetic Fields, Mass. Inst. of Technology, November 1961.

6. LUPTON, W.H. 'Fast triggered spark switches for a two megajoule capacitor bank', Proc. Fifth Int. Conf. on Ionization Phenomena in Gases, Munich, 1961.

7. KEMP, E.L. and QUINN, W.E. 'The power crowbar energy system for Scylla IV, 3rd Symposium on Engineering Problems in Thermonuclear Research, Munich, 1964, p.70.

8. BAYES, D.V., HUCKLESBY, R.J. and WARD, B.J. 'A passive crowbar for the 1 - MJ thetatron using 32 solid dielectric switches in parallel', 4th Symposium on Engineering Problems in Thermonuclear Research, Rome, 1966.

9. FITCH, R.A. and McCORMICK, N.R. 'Low inductance switching using parallel sparkgaps', Proc. IEE, 1959, 106A, Suppl. 2, p.117.

10. FITCH, R.A. and McCORMICK, N.R. 'The modes of operation of a cascade spark-gap for precision switching', Proc. 4th Int. Conf. on Ionization Phenomena in Gases, Uppsala, p.463, 1959.

11. STREET, J.C. and BEAMS, J.W. 'The fall of potential in the initial stages of electrical discharges', Phys. Rev. 1931, 38, p.416.

12. FLETCHER, R.C. 'Impulse breakdown in the 10^{-9} second range of air at atmospheric pressure', Phys. Rev. 1949, 76, No.10, p.1501.

13. REYNOLDS, J.A., ALDRIDGE, E.E., KEILHACKER, M. and NIBLETT, G.B.F. 'Control of plasma drift in the thetatron', Physics of Fluids (USA) 1965, 8, No.3, p.529.

14. BREWSTER, D.W. and NESSIM, A.F. 'The thetatron: shock wave problems in the design of the equipment', Concrete and Constructional Engineering 1966, LX1, No.6, p.205.

15. NIBLETT, G.B.F. 'The thetatron experiment', Concrete and Constructional Engineering, 1966, LX1, No.7, p.251.

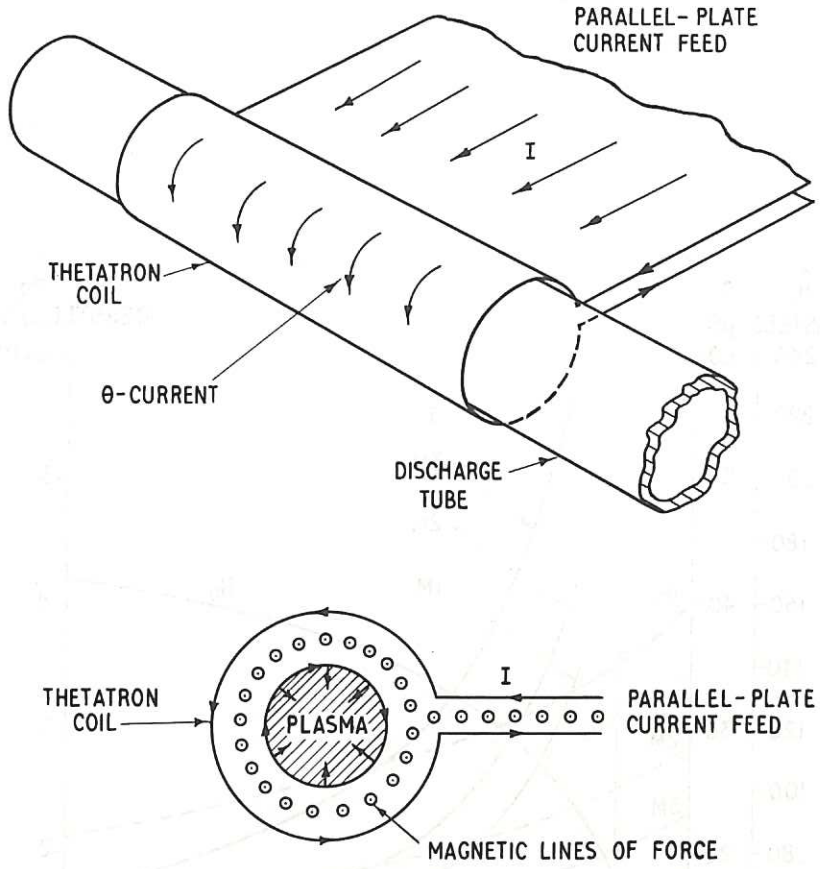

Fig. 1 Simplified diagram of thetatron experiment (CLM-P 130)

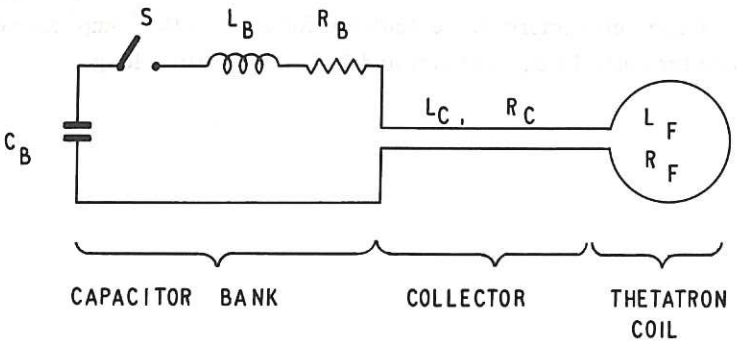

Fig. 2 Simplified circuit of large capacitor bank (CLM-P 130)

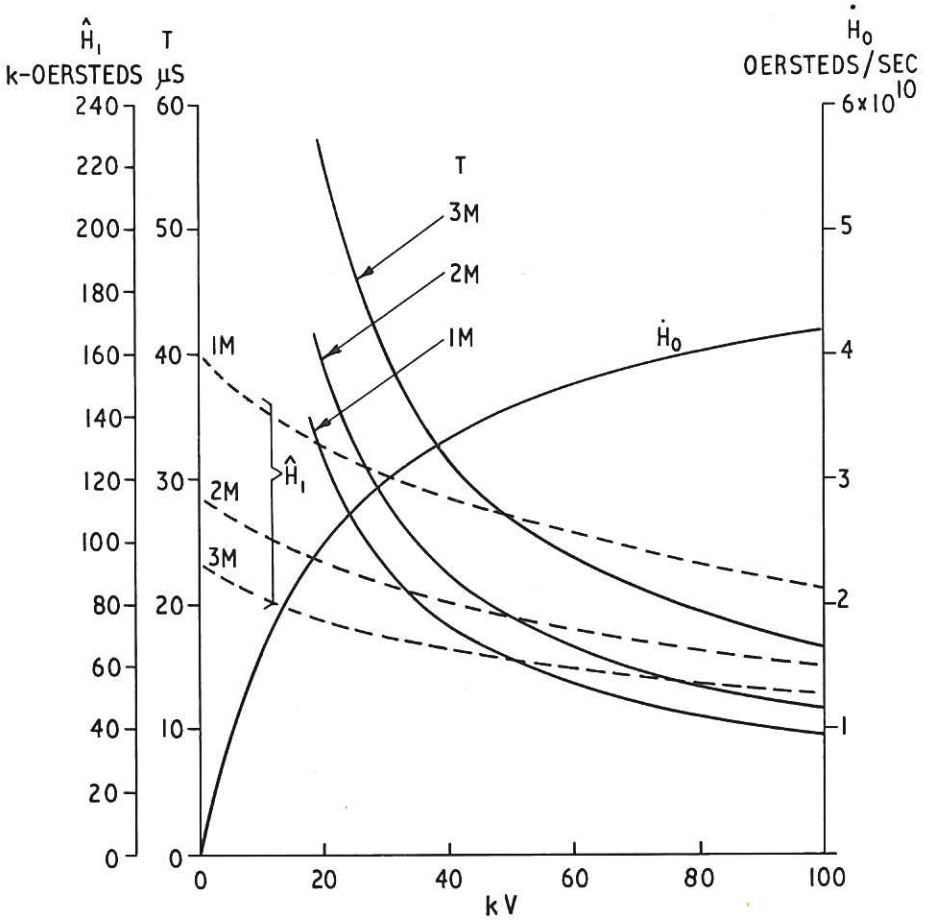

Fig. 3 (CLM-P 130)

Predicted MJ bank characteristics calculated for $k = 4 \times 10^{10}$ amp/cm/sec and for coils 10 cm diameter and 1, 2 and 3 metres long

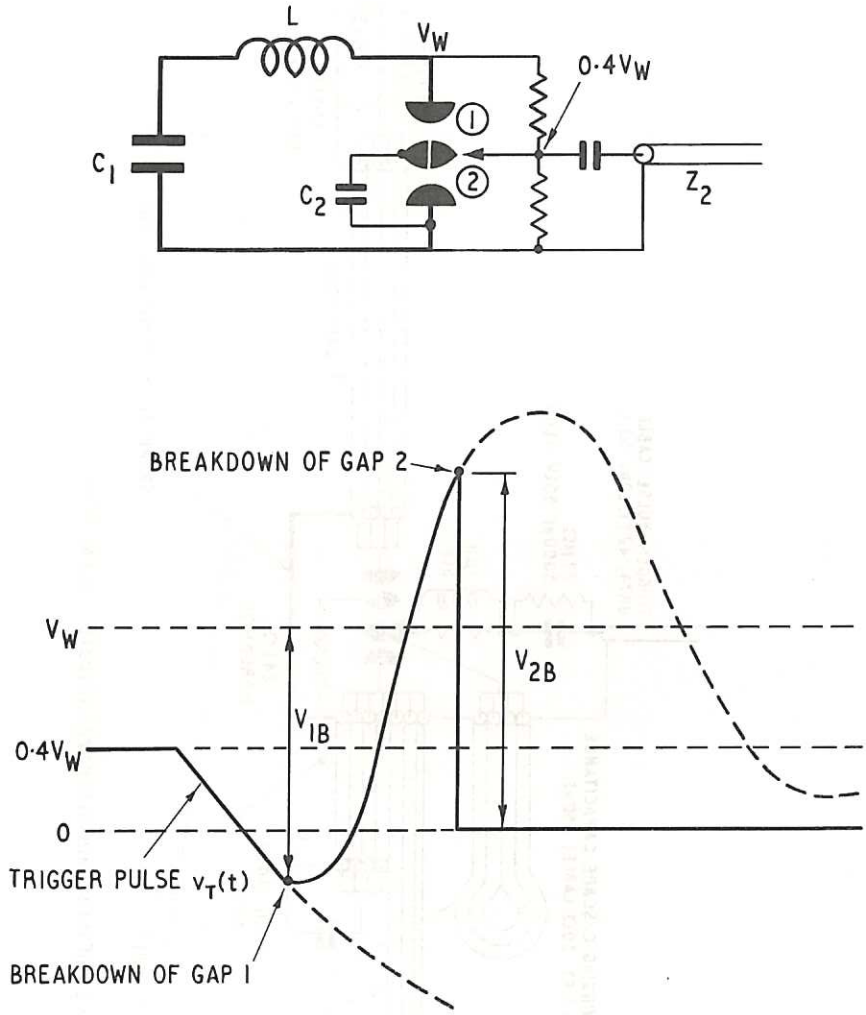

Fig. 4 (CLM-P 130)
Swinging cascade sparkgap: (a) simplified circuit diagram;
(b) schematic trigger-electrode waveform

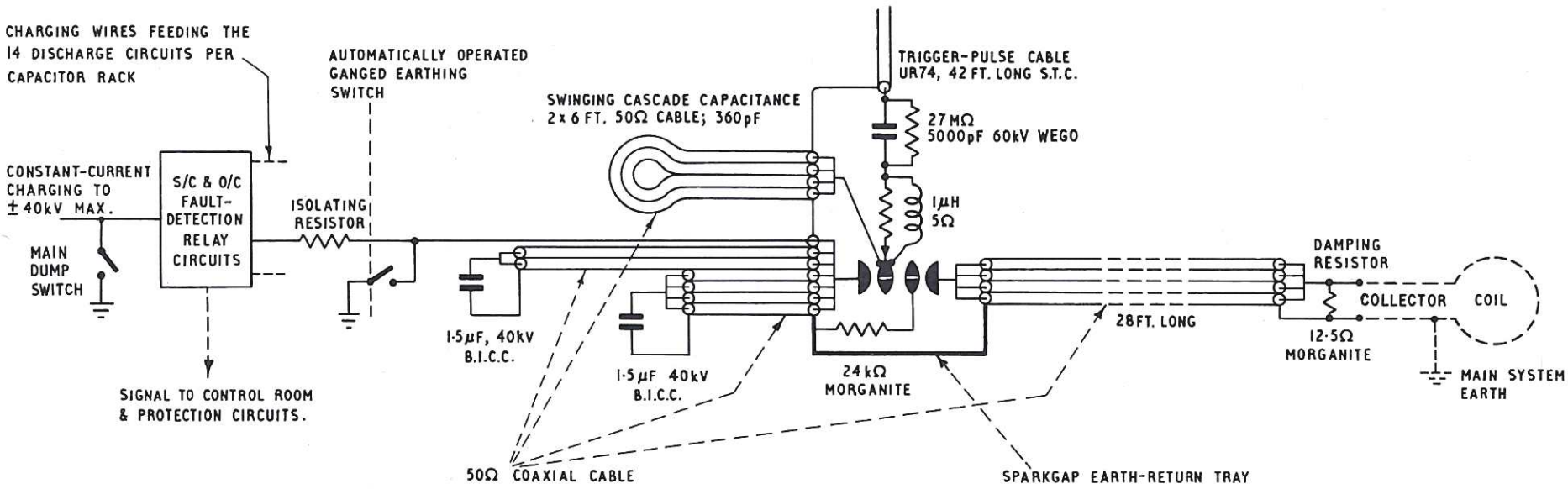

Fig. 5 Details of one main-discharge circuit (CLM-P 130)

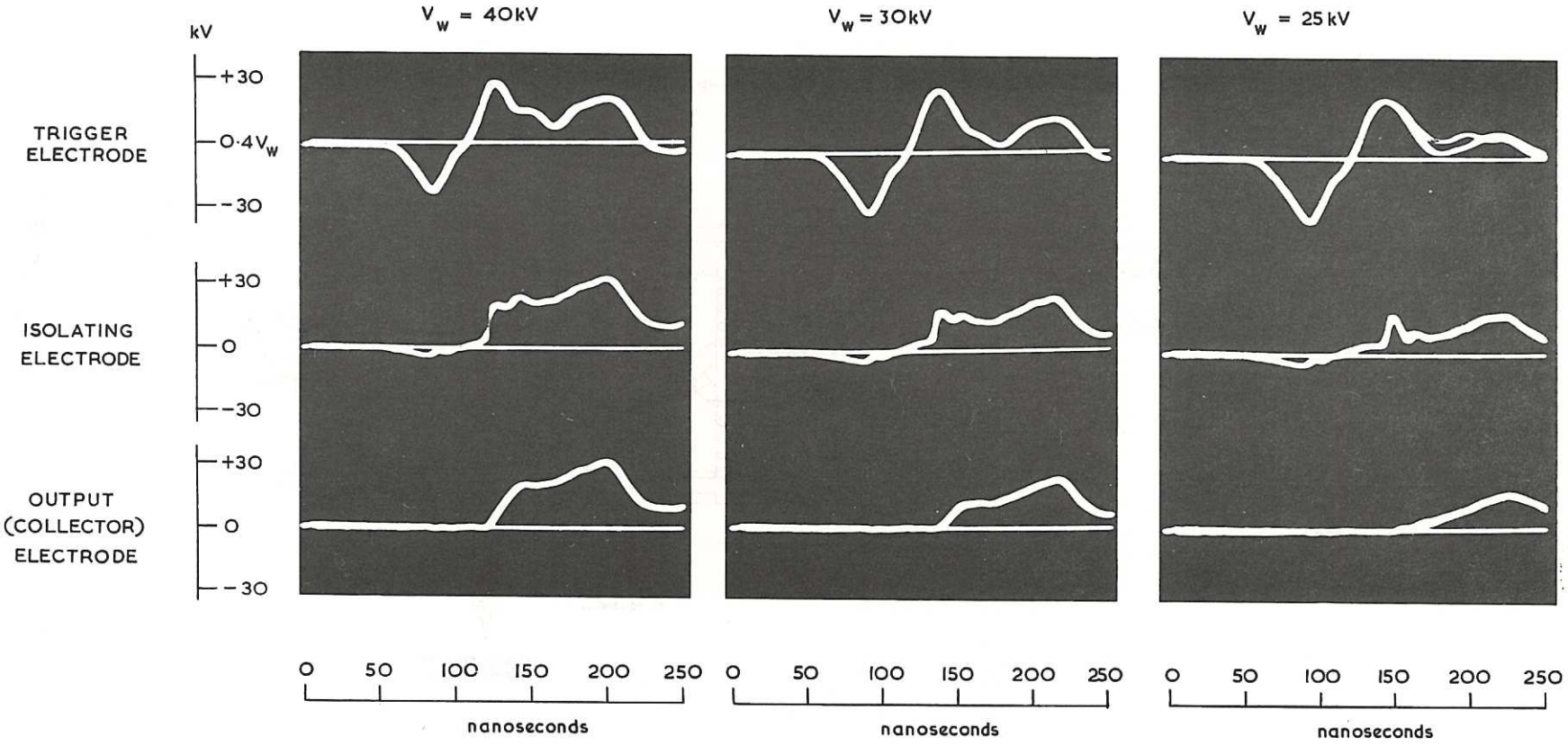

Fig. 6 (CLM-P 130)

Main-sparkgap waveforms: electrode waveforms covering the normal voltage range (30-40 kV) and the lower test voltage (25 kV)

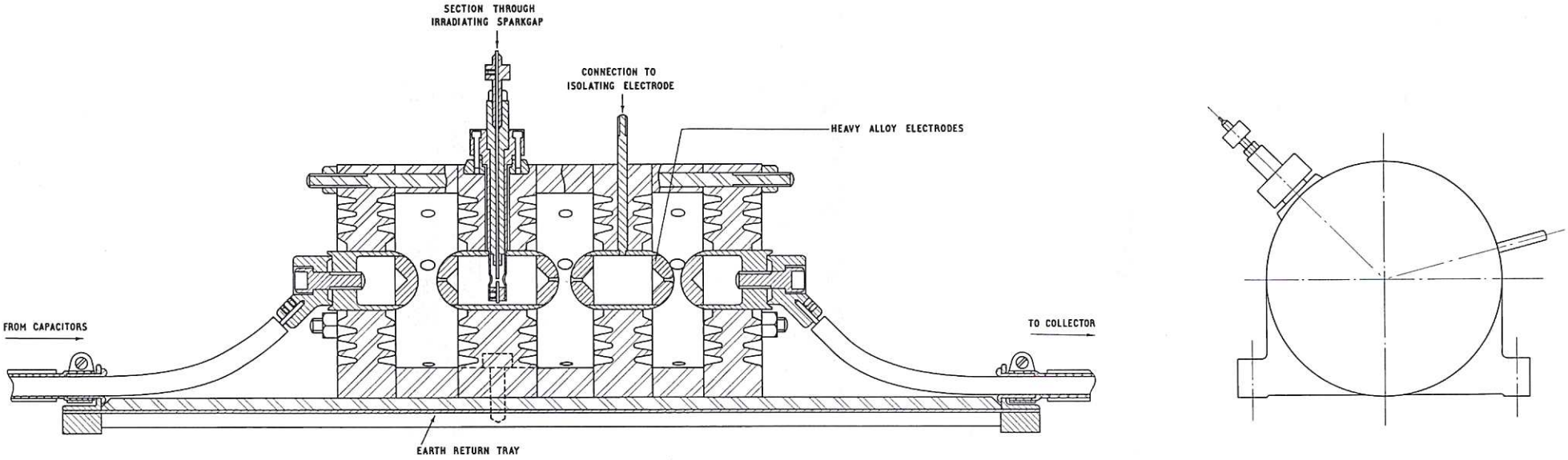

Fig. 7 Mechanical details of a main sparkgap (CLM-P 130)

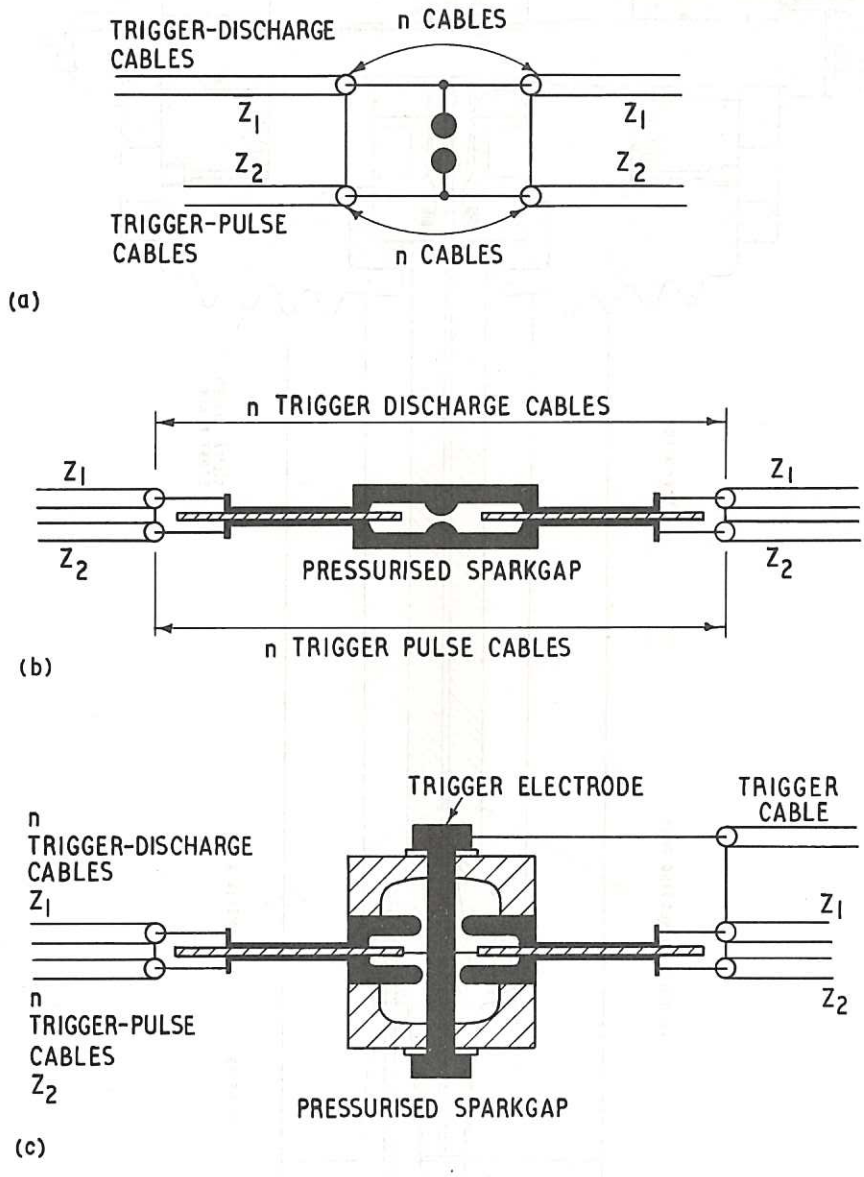

Fig. 8 (CLM-P130)

Sparkgaps for trigger-pulse generators: (a) circuit diagram; (b) schematic diagram of a pressurised 2-electrode gap; (c) schematic diagram of a pressurised swinging-cascade gap

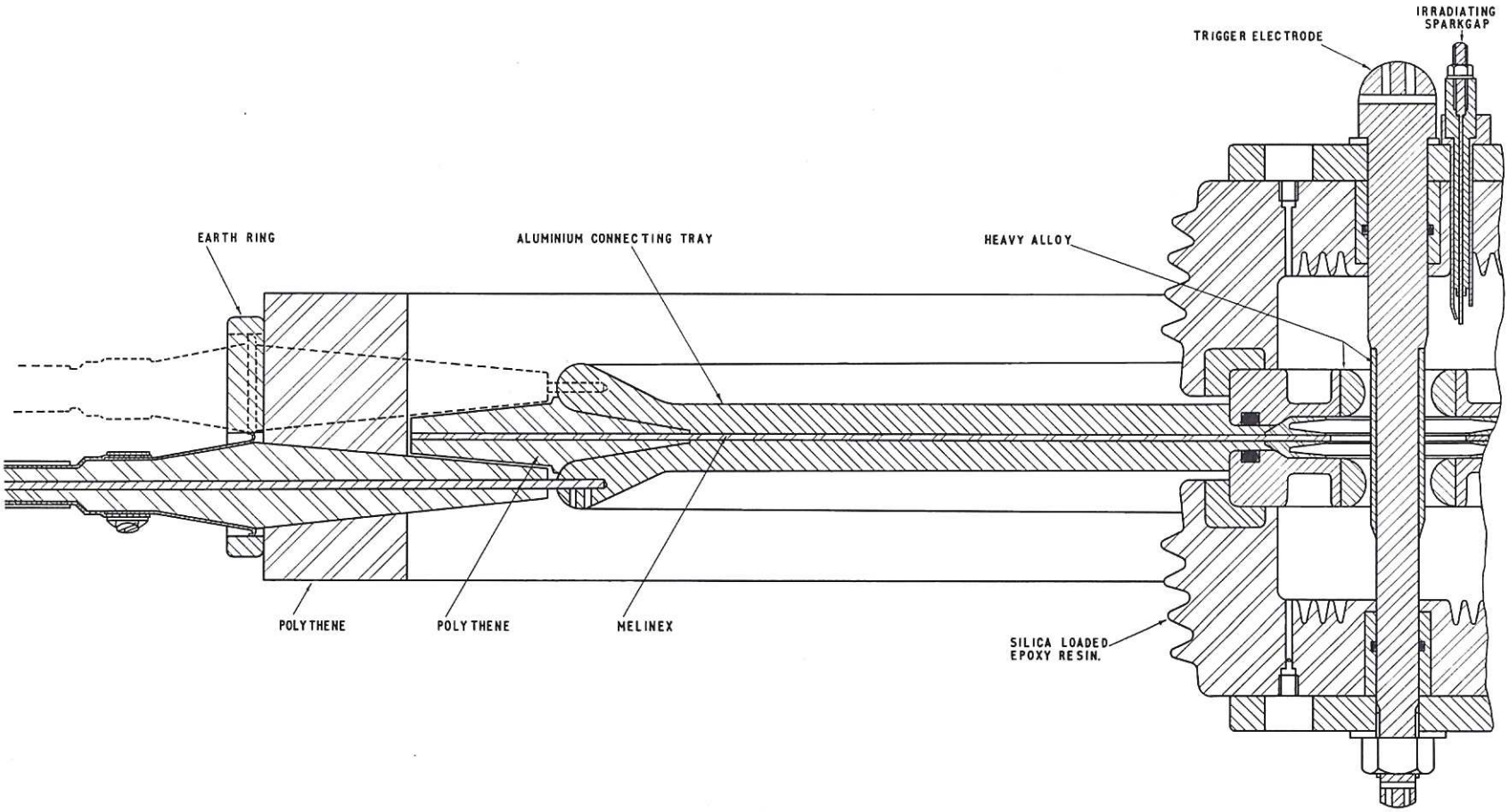

Fig. 9 (CLM-P 130)
Mechanical details of a pressurised swinging-cascade sparkgap for a sub-master trigger-pulse generator

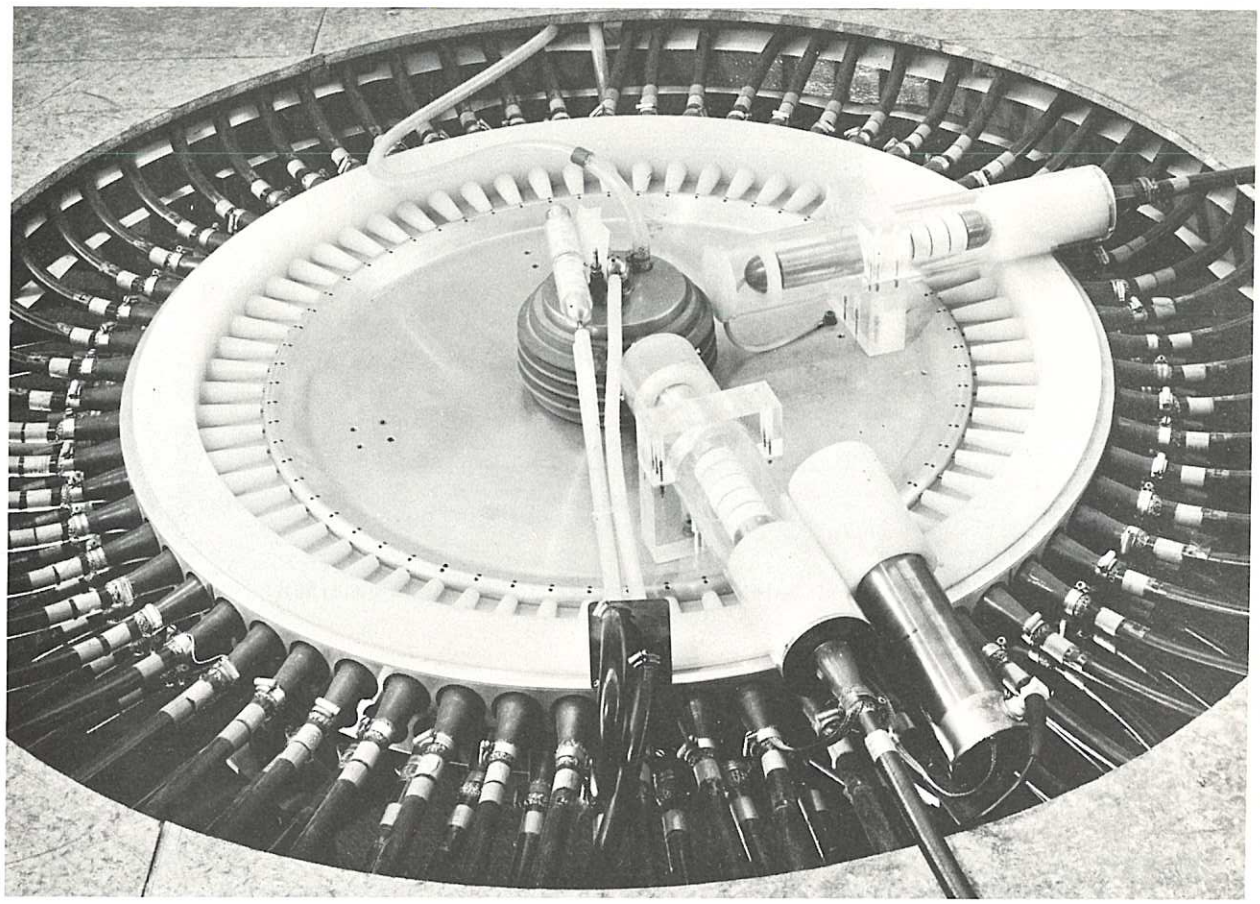

Fig. 10 Photograph of an assembled sub-master trigger-pulse generator (CLM-P 130)

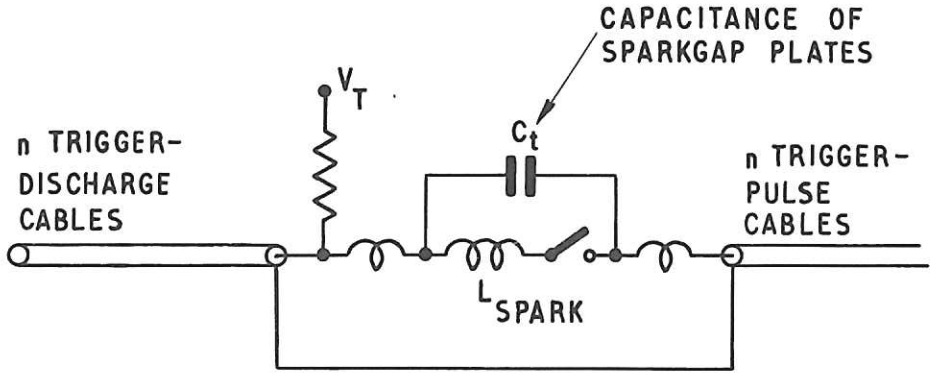

Fig. 11 Equivalent circuit of trigger-pulse generator (CLM-P 130)

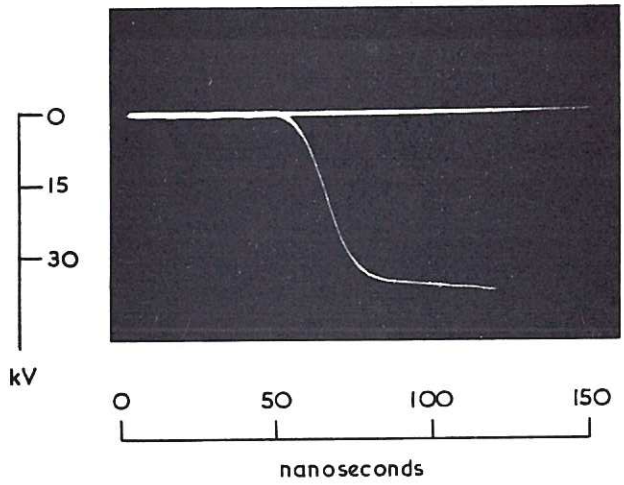

Fig. 12 (CLM-P 130)
Open-circuit output pulse from sub-master trigger-pulse generator

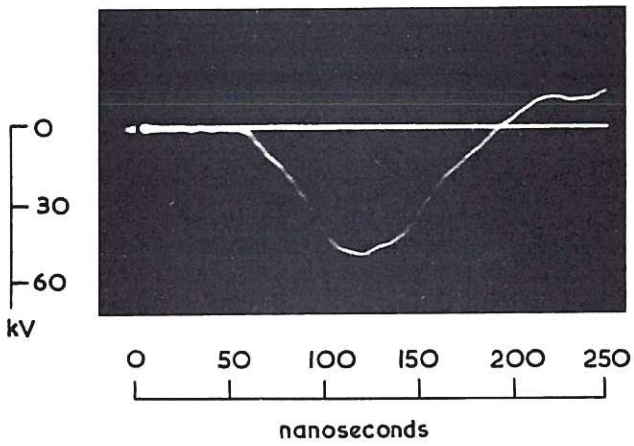

Fig. 13 Trigger-pulse waveform at main sparkgap (CLM-P 130)

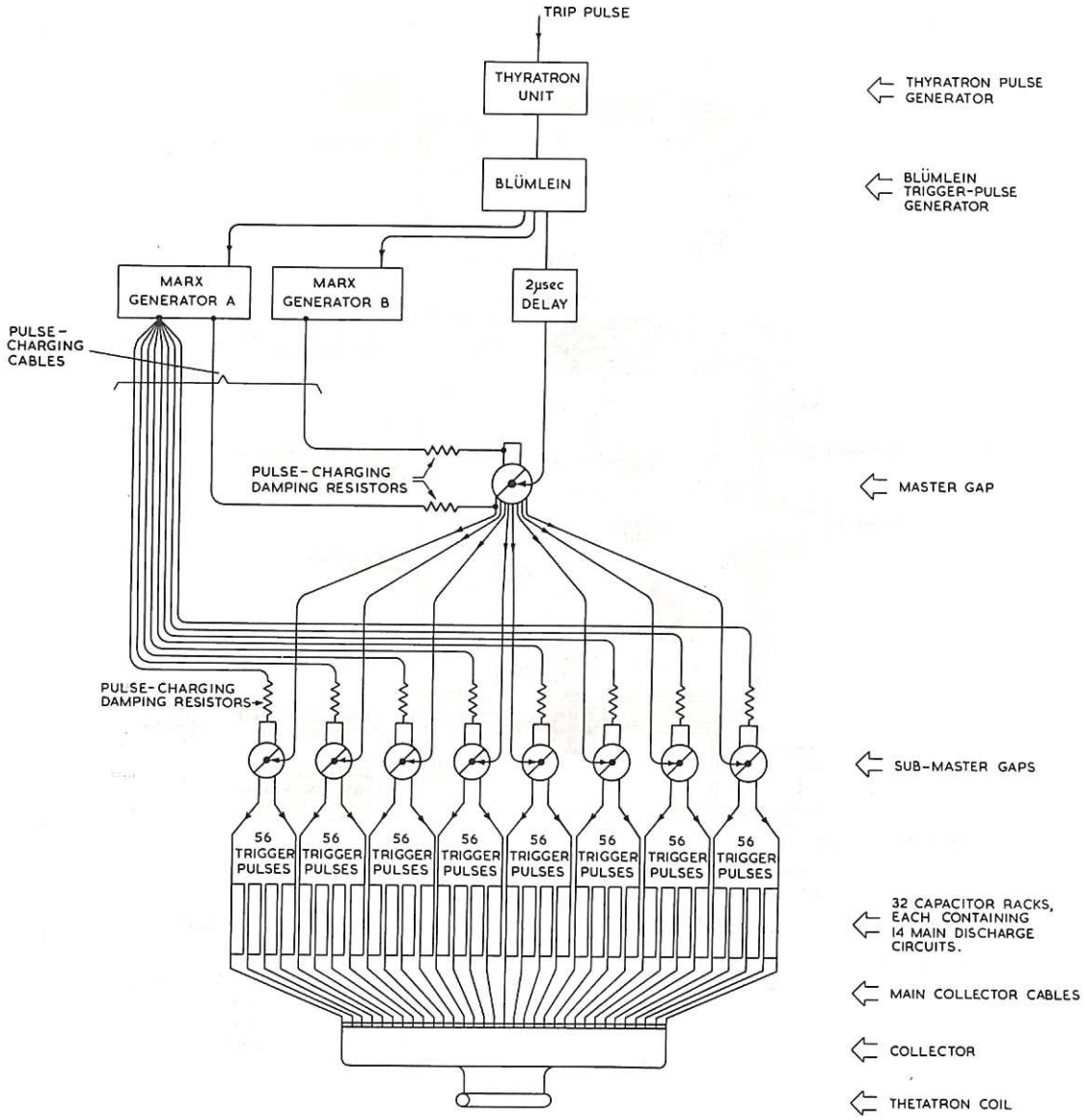

Fig. 14 Schematic diagram of the MJ bank circuit (CLM-P 130)

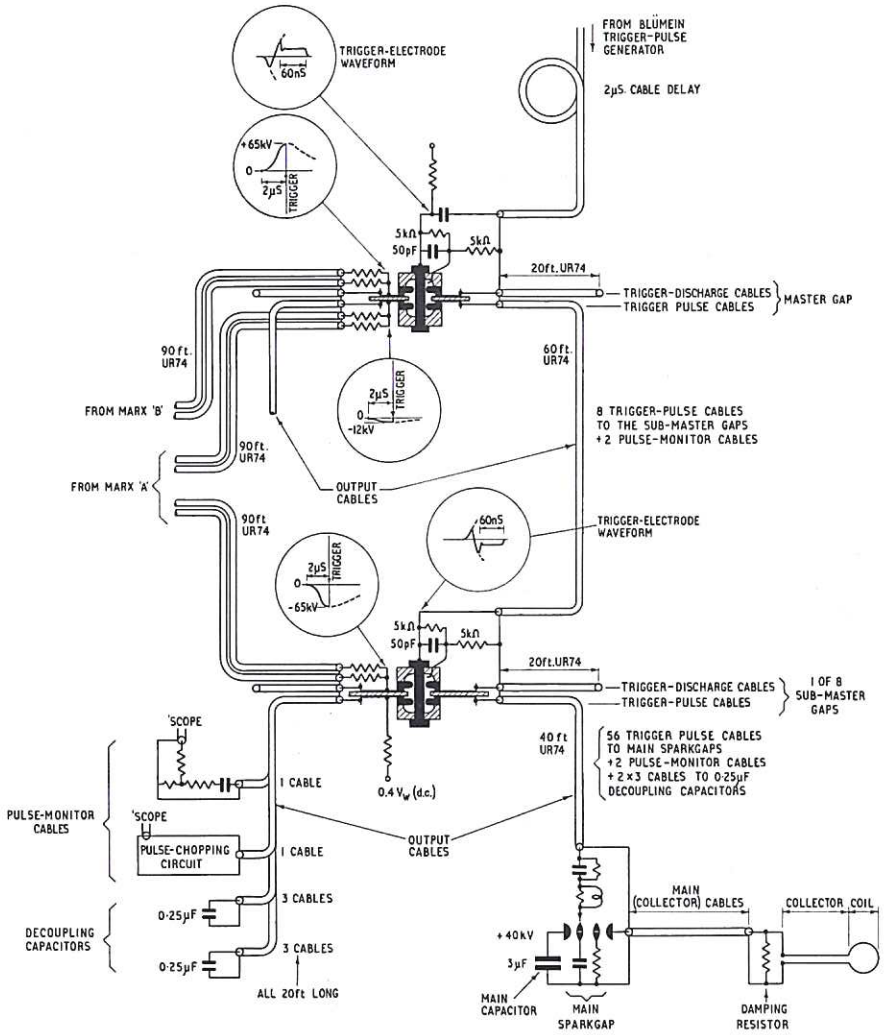

Fig. 15 Details of the MJ bank trigger circuit (CLM-P 130)

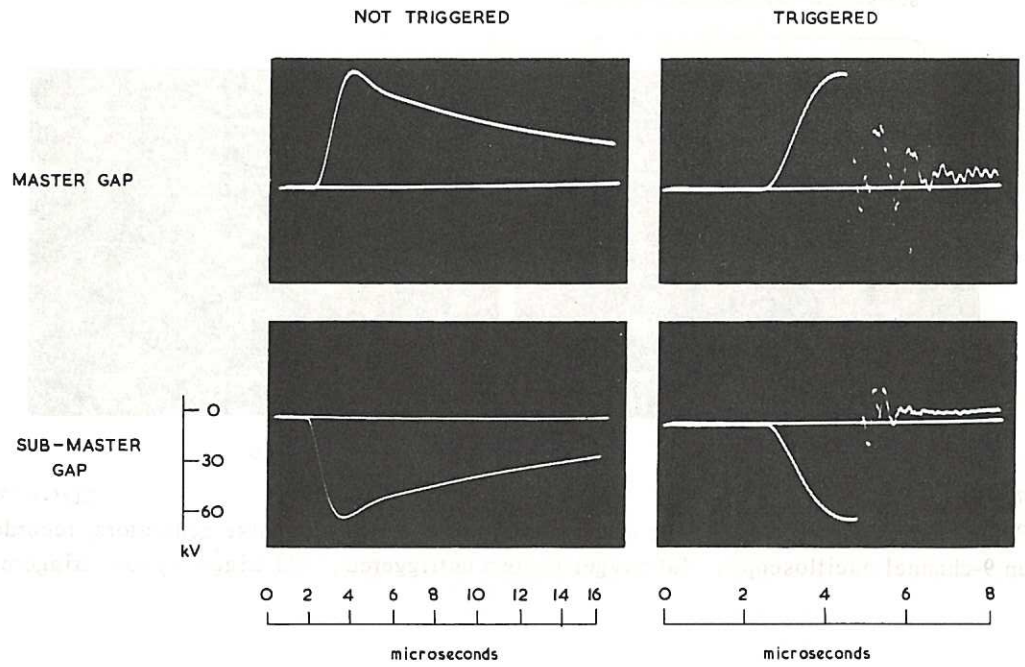

Fig. 16 Pulse-charging waveforms in the trigger system (CLM-P 130)

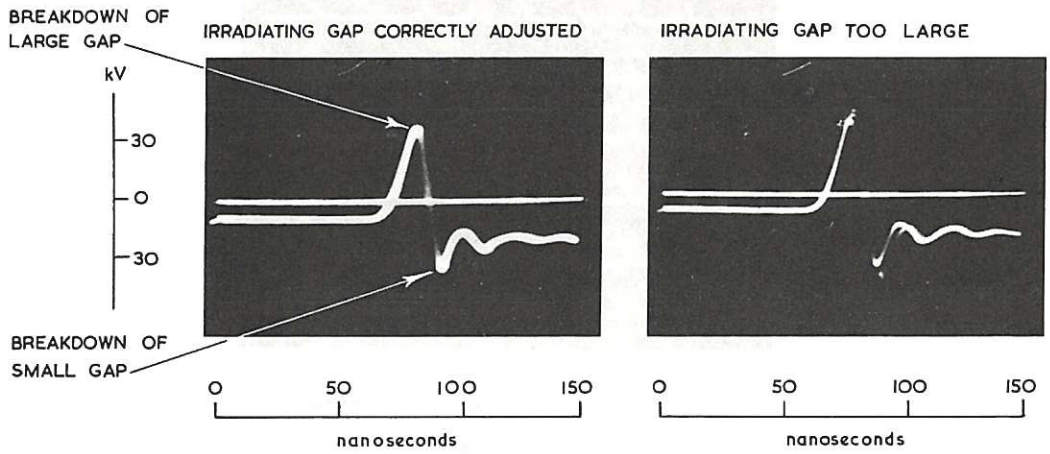

Fig. 17 Five superimposed trigger-electrode waveforms of a sub-master gap (CLM-P 130)

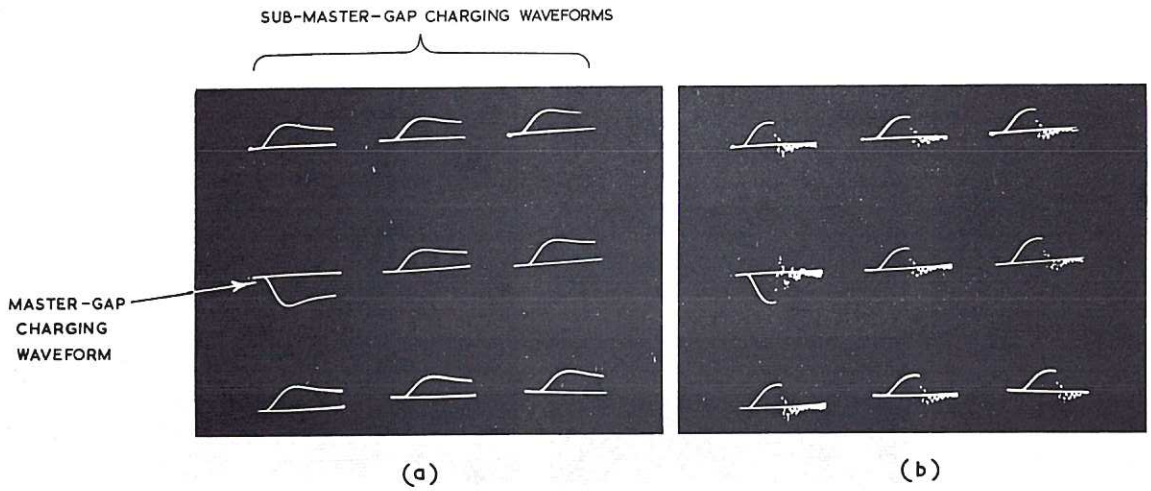

Fig. 18 (CLM-P 130)

Pulse-charging waveforms for the master and sub-master trigger-pulse generators, recorded on 9-channel oscilloscope; (a) trigger system untriggered; (b) trigger system triggered

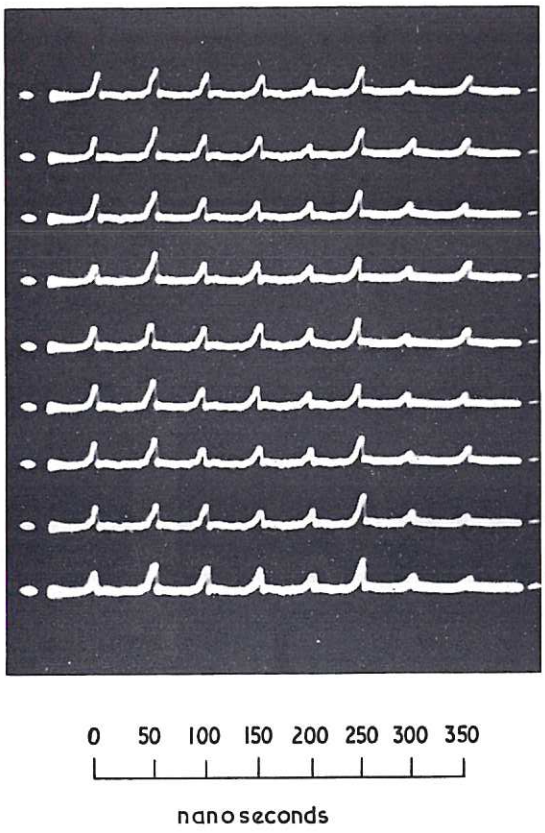

Fig. 19 (CLM-P 130)

Consecutive records of voltage spikes indicating the relative breakdown times of trigger-pulse-generator sparkgaps

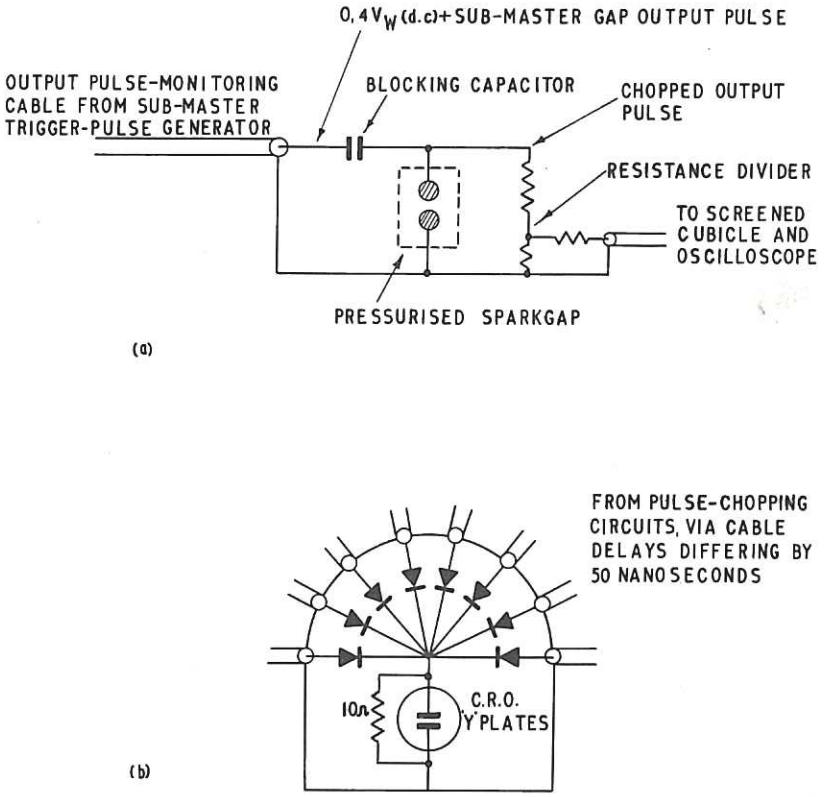

Fig. 20 (CLM-P 130)
Circuits for deriving and displaying voltage spikes from trigger pulses
(a) pulse-chopping circuit; (b) oscilloscope input circuit

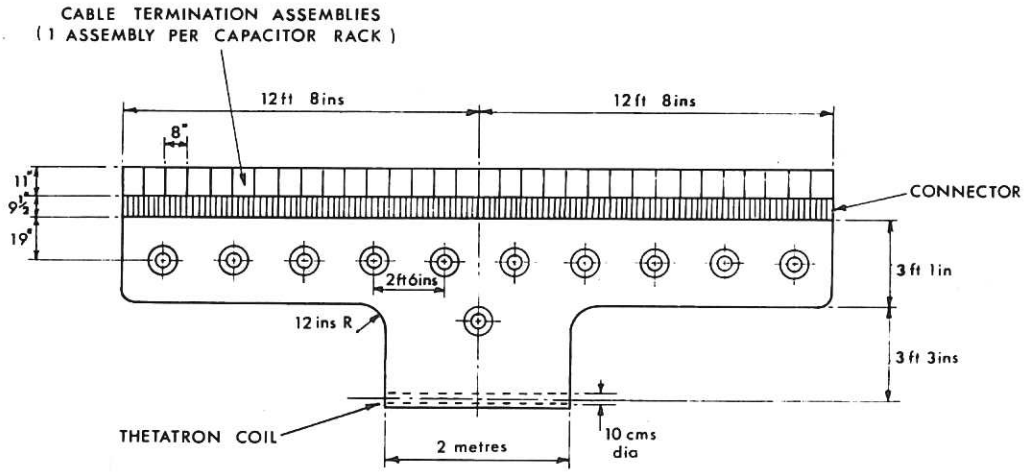

Fig. 21 Plan of collector (CLM-P 130)

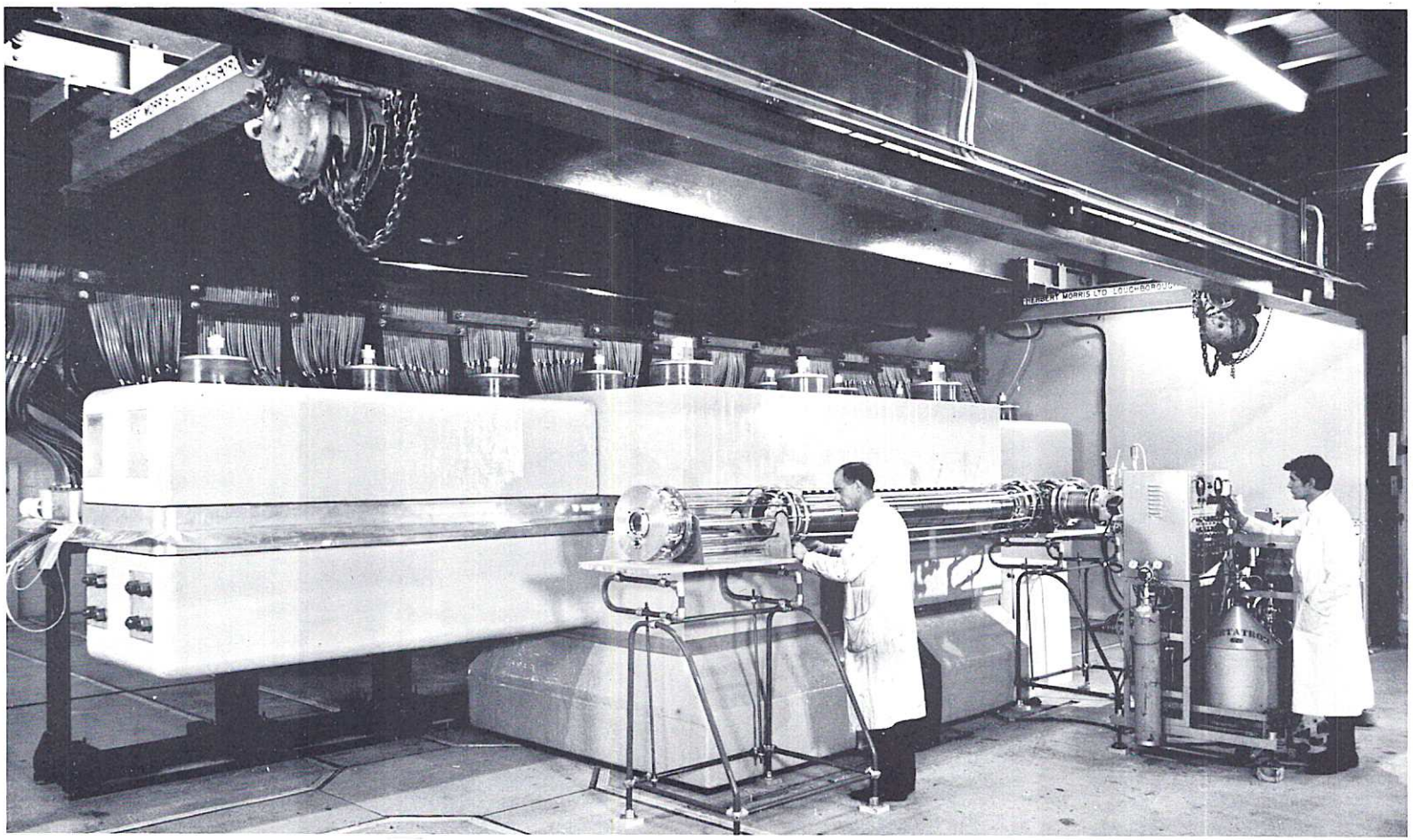

Fig. 22 Photograph of the collector and coil assembly in the experimental area (CLM-P 130)

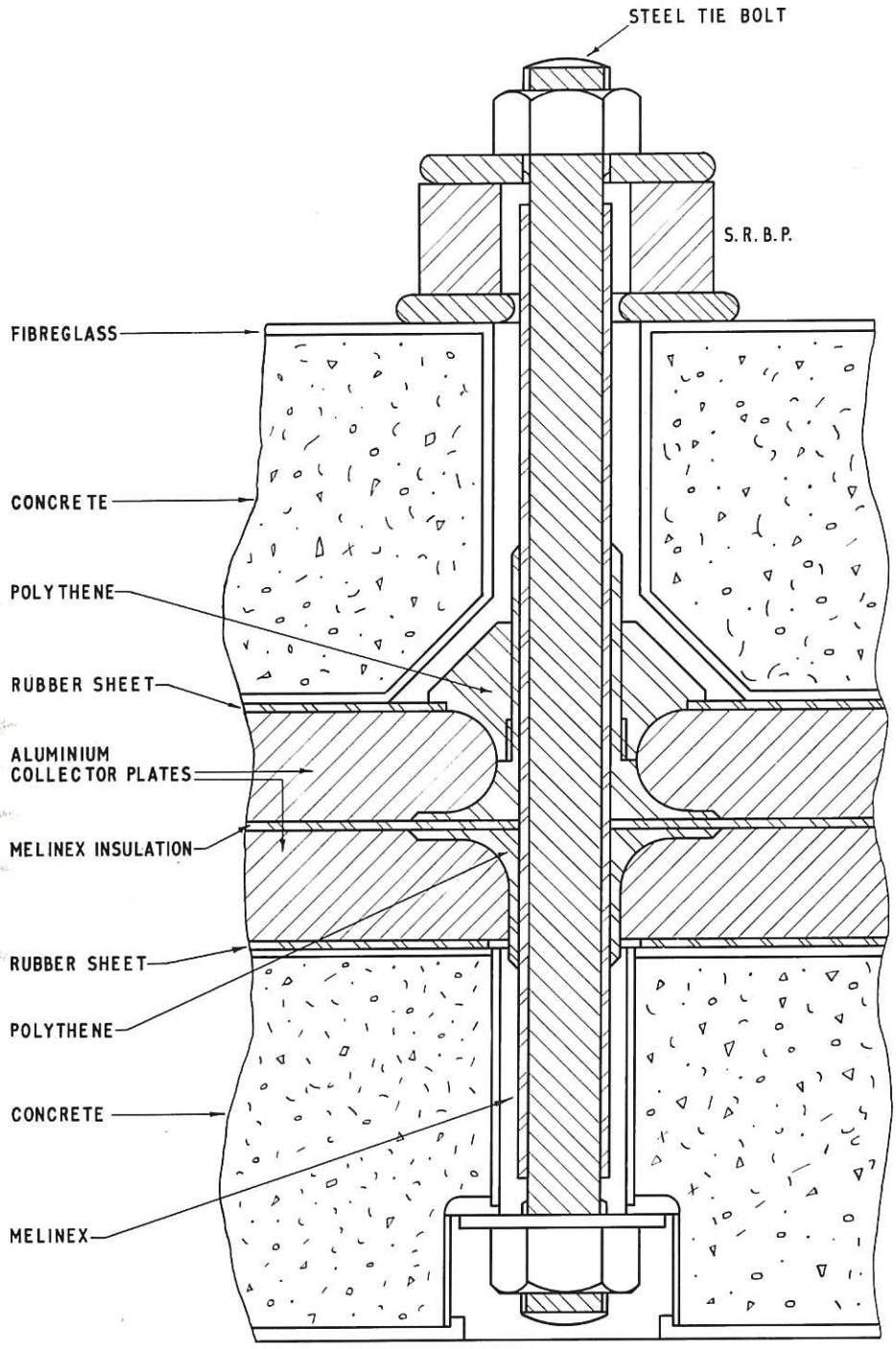

Fig. 23 Cross-section through collector at a tie bolt (CLM-P 130)

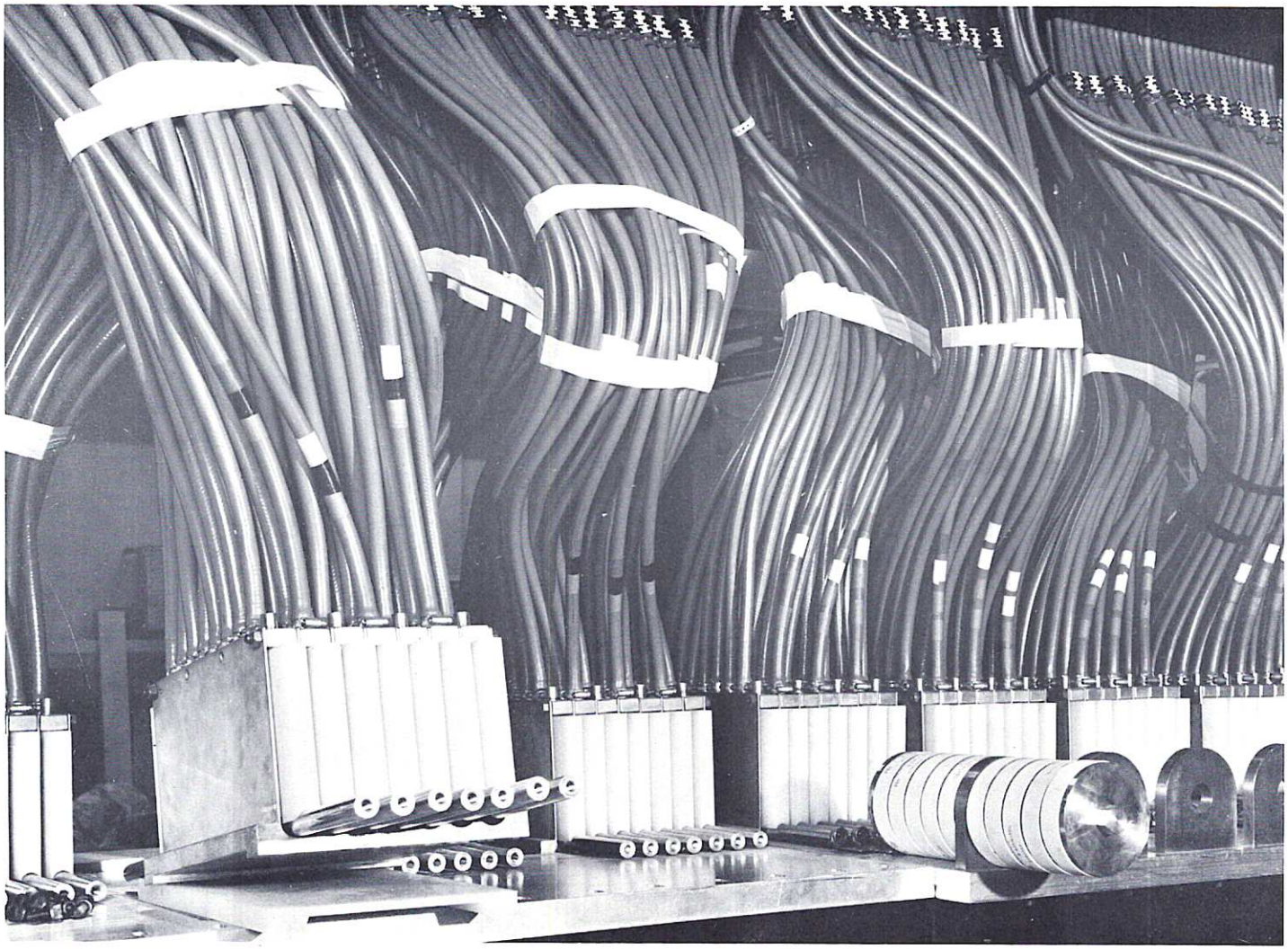

Fig. 24 Photograph of the rear face of the collector during assembly (CLM-P 130)

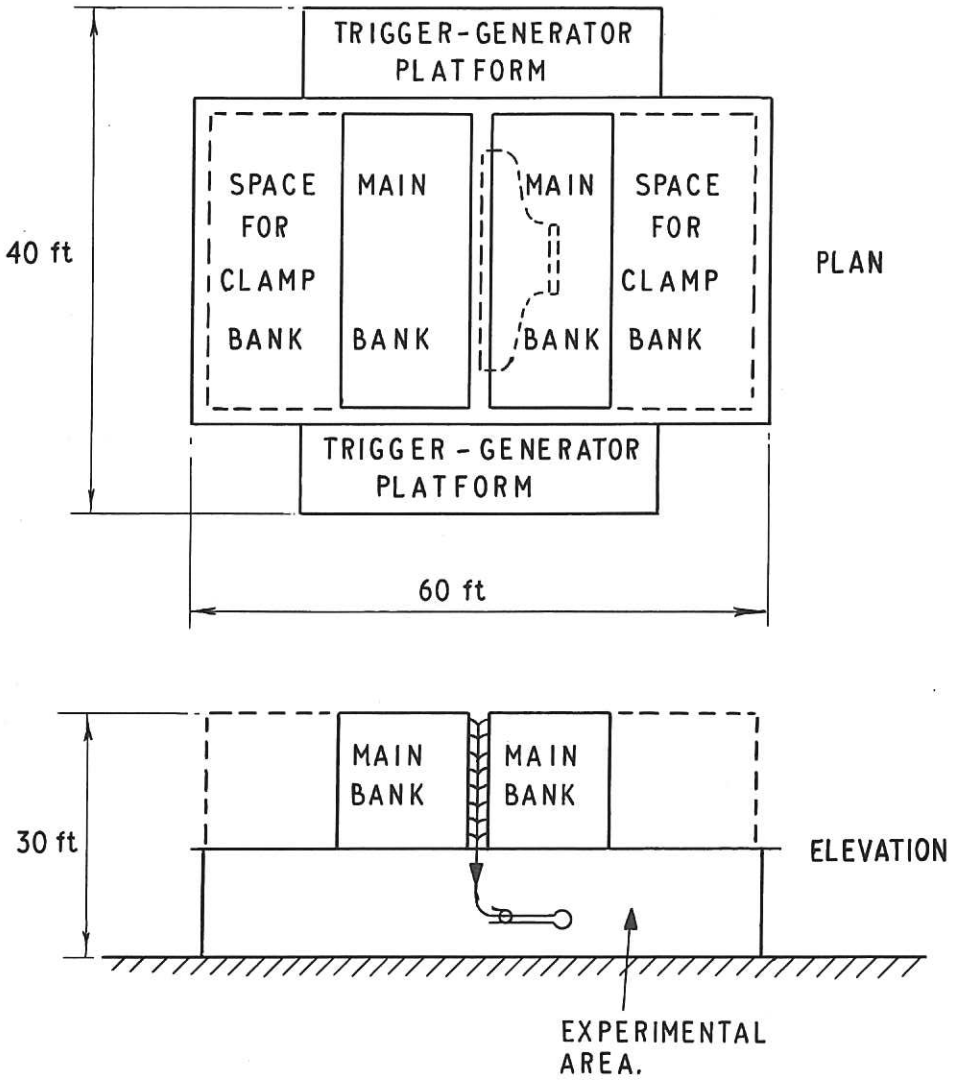

Fig. 25 Schematic diagram of the megajoule-bank layout (CLM-P 130)

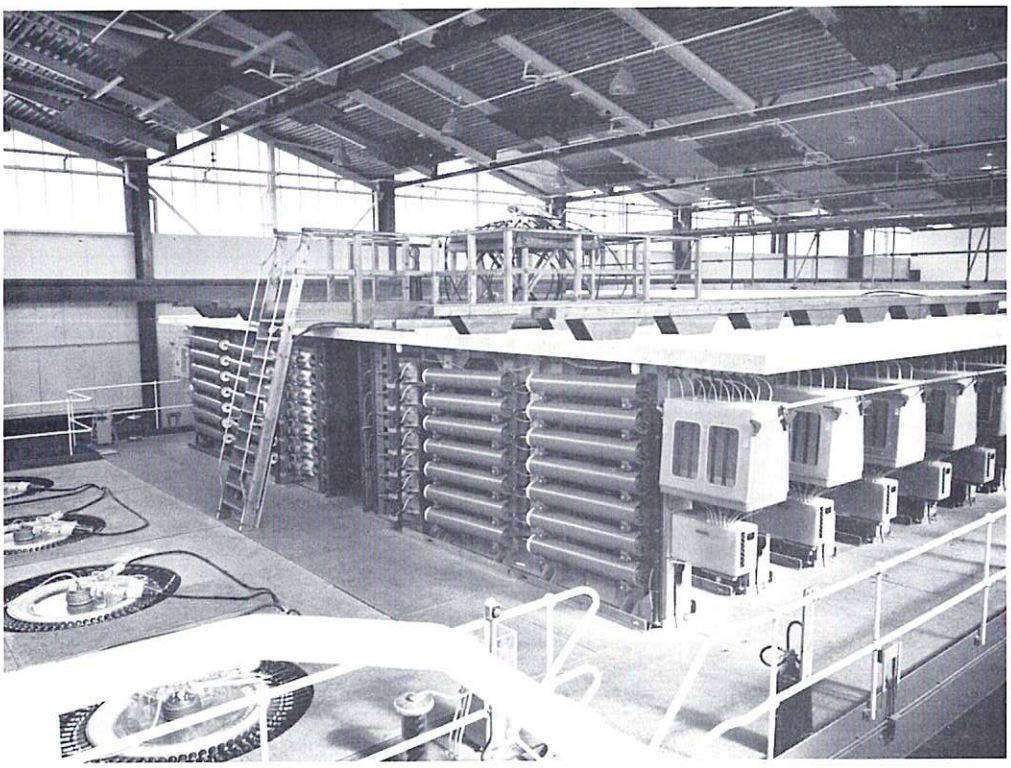

Fig. 26 Photograph of the top floor of the megajoule bank (CLM-P 130)

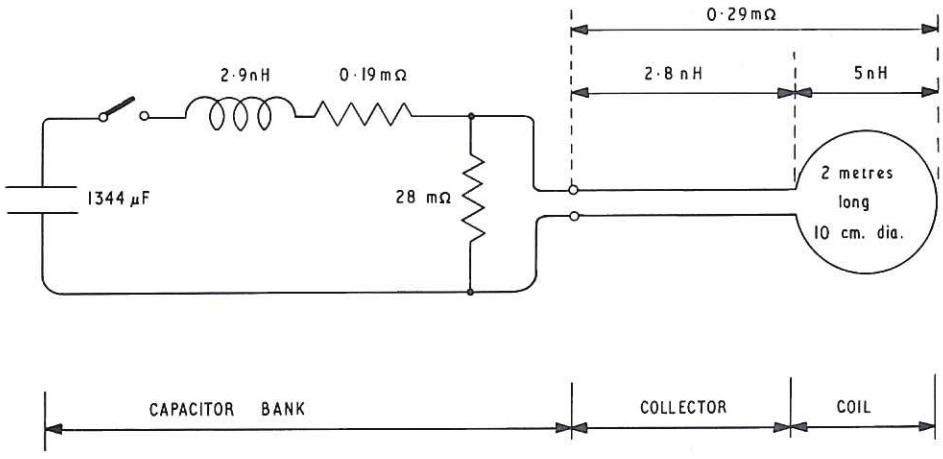

Fig. 27 Measured circuit parameters of the megajoule bank (CLM-P 130)